

¹ The Evolution of Siphonophore Tentilla as Specialized Tools for Prey Capture

³ Alejandro Damian-Serrano^{1,‡}, Steven H.D. Haddock², Casey W. Dunn¹

⁴ ¹ Yale University, Department of Ecology and Evolutionary Biology, 165 Prospect St.,
⁵ New Haven, CT 06520, USA

⁶ ² Monterey Bay Aquarium Research Institute, 7700 Sandholdt Rd., Moss Landing, CA
⁷ 95039, USA

⁸ [‡] Corresponding author: Alejandro Damian-Serrano, email: alejandro.damianserrano@
⁹ yale.edu

¹⁰ Abstract

¹¹ Predators have evolved dedicated body parts to capture and subdue prey. As different
¹² predators specialize on distinct prey taxa, their tools for prey capture diverge into a variety
¹³ of adaptive forms. Studying the evolution of predation is facilitated by a predator clade
¹⁴ with structures used exclusively for prey capture and with significant morphological varia-
¹⁵ tion. Siphonophores, a clade of colonial cnidarians, satisfy these criteria particularly well,
¹⁶ capturing prey with their tentilla (tentacle side branches). Earlier work has shown that
¹⁷ extant siphonophore diets correlate with the different morphologies and sizes of their tentilla
¹⁸ and nematocysts. We hypothesize that evolutionary specialization on different prey types
¹⁹ has driven the phenotypic evolution of these characters. To test this hypothesis, we: (1)
²⁰ measured multiple morphological traits from fixed siphonophore specimens using microscopy
²¹ and high-speed video techniques, (2) built a phylogenetic tree of 45 species, and (3) analyzed
²² the evolutionary associations between siphonophore nematocyst characters and prey type
²³ data from the literature. Our results show that siphonophore tentillum structure has strong
²⁴ evolutionary associations with prey type and size specialization, and suggest that shifts
²⁵ between prey-type specializations are linked to shifts in tentillum and nematocyst size and
²⁶ shape. We found that predatory specialists can evolve into generalists, and that specialists on
²⁷ one prey type have directly evolved into specialists on other prey types. Thus, the evolutionary
²⁸ history of tentilla shows that siphonophores are an example of ecological niche diversification
²⁹ via morphological innovation and evolution. This study contributes to understanding how
³⁰ morphological evolution has shaped present-day oceanic food webs.

³¹ Keywords

³² Siphonophores, tentilla, nematocysts, predation, specialization, character evolution

³³

³⁴ Most animal predators have characteristic biological tools that they use to capture and
³⁵ subdue prey. Raptors have claws and beaks, snakes have fangs, wasps have stingers, and
³⁶ cnidarians have nematocyst-laden tentacles. The functional morphology of these structures
³⁷ tend to be finely attuned to their ability to successfully capture specific prey (Schmitz

38 2017). Long-term adaptive evolution in response to the defense mechanisms of the prey (*e.g.*
39 avoidance, escape, protective barriers) leads to modifications that can counter those defenses
40 The more specialized the diet of a predator is, the more specialized its tools need to be to
41 meet the specific challenges posed by the prey. Understanding the relationships between
42 predatory specializations and morphological specializations is necessary to contextualize the
43 phenotypic diversity of predators, and to quantify the importance of ecological diversification
44 in generating this diversity.

45 Siphonophores (Cnidaria : Hydrozoa) are a clade of organisms bearing modular structures
46 that are exclusively used for prey capture: the tentilla (Fig. 1). These present a significant
47 morphological variation across species (Mapstone 2014) (Fig. 2), which makes them an
48 ideal system to study the relationships between functional traits and prey specialization. A
49 siphonophore is a colony bearing many feeding polyps (Fig. 1), each with a single tentacle,
50 which branches into several tentilla carrying the functional cnidocytes (specialized neural cells
51 carrying nematocysts, the stinging capsules). Unlike most other cnidarians, siphonophores
52 carry their tentacle nematocysts in extremely complex and organized batteries (Skaer 1988)
53 built into their tentilla. While nematocyst batteries and clusters in other cnidarians are simple
54 static scaffolds for cnidocytes, siphonophore tentilla have their own reaction mechanism,
55 triggered upon encounter with prey. When it fires, a tentillum undergoes an extremely
56 fast conformational change that wraps it around the prey, maximizing the surface area
57 of contact for nematocysts to fire on the prey (Mackie et al. 1987). In addition, some
58 species have elaborate fluorescent and bioluminescent lures on their tentilla to attract prey
59 with aggressive mimicry (Purcell 1980; Haddock et al. 2005; Haddock and Dunn 2015).
60 Siphonophores bear four major nematocyst types in their tentacles and tentilla. The largest
61 type, heteronemes, have open-tip tubules characterized by bearing a distinctly wider spiny
62 shaft at the proximal end of the everted tubule. These are typically found flanking the
63 proximal end of the cnidoband. The most abundant type, haplonemes, have no distinct shaft,
64 but similarly to heteronemes, their tubules have open tips and can be found in the cnidoband.
65 Both heteronemes and haplonemes bear short spines along the tubule and can be toxic and
66 penetrate the surface of some prey types. In the terminal filament, siphonophores bear two
67 other types of nematocysts, characterized by their adhesive function, closed tip tubules, and
68 lack of spines on the tubule. These are the desmonemes (a type of adhesive coiled-tubule
69 spironeme), and rhopalonemes (a siphonophore-exclusive nematocyst type with wide tubules).

70 Many siphonophore species inhabit the deep pelagic ocean, which spans from ~200m to
71 the oceanic seafloor. This habitat has fairly homogeneous physical conditions and stable
72 zooplankton abundances and composition (Robison 2004). With a relatively predictable
73 prey availability, ecological theory would predict evolution to drive coexisting siphonophore
74 lineages towards specialization, increasing their feeding efficiencies and reducing interspecific
75 competition (Simpson 1944; Hardin 1960; Hutchinson 1961). If this prediction holds true,
76 we expect the prey capture apparatus morphologies of siphonophores to diversify with the
77 evolution of increased specialization on a variety of prey types in different siphonophore
78 lineages.

79 Specialization is often thought to be an evolutionary ‘dead end’, meaning that specialized
80 lineages are unlikely to evolve into generalists or to shift the resource for which they are
81 specialized (Futuyma and Moreno 1988). However, recent studies have found that interspecific
82 competition can favor the evolution of resource generalism (Stireman-III 2005; Johnson et

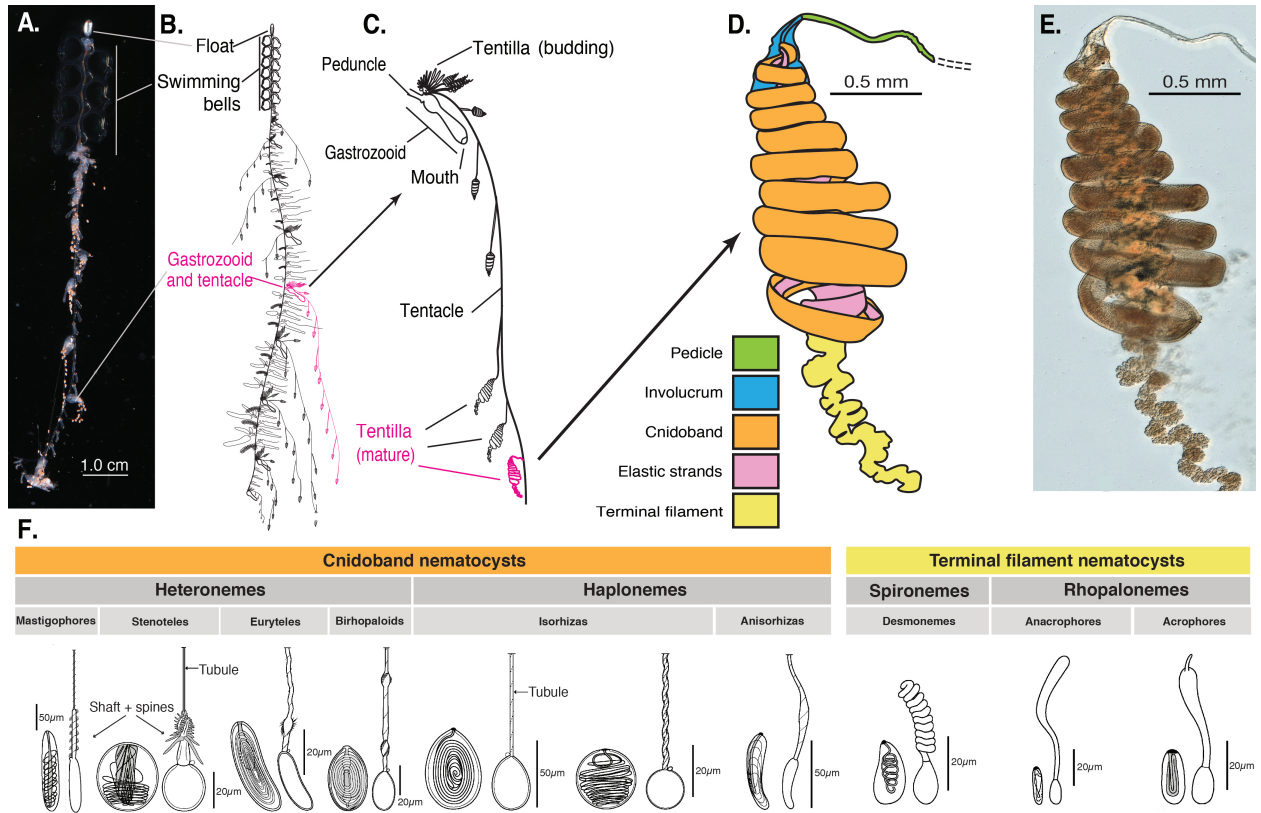


Figure 1: Siphonophore anatomy. A - *Nanomia* sp. siphonophore colony (photo by Catriona Munro). B,C - Illustration of a *Nanomia* colony, gastrozooid, and tentacle (by Freya Goetz). D - *Nanomia* sp. Tentillum illustration and main parts. E - Differential interference contrast micrograph of the tentillum illustrated in D. F - Nematocyst types (illustration reproduced with permission from Mapstone 2014), hypothesized homologies, and locations in the tentillum. Undischarged to the left, discharged to the right.

83 al. 2009) and resource switching (Hoberg and Brooks 2008). Here we examine three
84 alternative hypotheses on siphonophore trophic specialization: (1) predatory specialists
85 evolved from generalist ancestors; (2) predatory specialists evolved from ancestral predators
86 which specialized on a different resource, switching their primary prey type; and (3) predatory
87 generalists evolved from specialist ancestors.

88 The study of siphonophore tentilla and diets has been limited in the past due to the
89 inaccessibility of their oceanic habitat and the difficulties associated with the collection of
90 fragile siphonophores. Thus, the morphological diversity of tentilla has only been characterized
91 for a few taxa, and their evolutionary history remains largely unexplored. Contemporary
92 underwater sampling technology provides an unprecedented opportunity to explore the trophic
93 ecology (Choy et al. 2017) and functional morphology (Costello et al. 2015) of siphonophores.
94 In addition, well-supported phylogenies based on molecular data are now available for these
95 organisms (Munro et al. 2018). These advances allow for the examination of relationships
96 between modern siphonophore form, function, and ecology, as well as reconstructing their
97 evolutionary history.

98 The few pioneering studies that have addressed the relationships between tentilla and
99 diet suggest that siphonophores are a robust system for the study of predatory specialization
100 via morphological diversification. (Purcell 1984) and (Purcell and Mills 1988) showed clear
101 relationships between diet, tentillum, and nematocyst characters in co-occurring epipelagic
102 siphonophores. These correlations, while studied for a small subset of extant epipelagic
103 siphonophore species, might be generalizable to all siphonophores. We hypothesize that
104 these relationships reflect correlated evolution between prey selection and tentillum (and
105 nematocyst) traits. Furthermore, we hypothesize that with an extensive characterization of
106 tentilla morphology, we can generate hypotheses about the diets of understudied siphonophore
107 species.

108 In this study, we characterize the morphological diversity of tentilla and their nematocysts
109 across a broad variety of shallow and deep sea siphonophore species using modern imaging
110 technologies, we expand the phylogenetic tree of siphonophores by combining a broad taxon
111 sampling of ribosomal gene sequences with a transcriptome-based backbone tree, and we
112 explore the evolutionary histories and correlations among diet, tentillum, and nematocyst
113 characters.

114 Methods

115 *Tentillum morphology* – The morphological work was carried out on siphonophore specimens
116 fixed in 4% formalin from the Yale Peabody Museum Invertebrate Zoology (YPM-IZ) collection
117 (accession numbers in Appendix 1). These specimens were collected intact across many years of
118 fieldwork expeditions, using blue-water diving (Haddock and Heine 2005), remotely operated
119 vehicles (ROVs), and human-operated submersibles. Tentacles were dissected from non-larval
120 gastrozooids, sequentially dehydrated into 100% ethanol, cleared in methyl salicylate, and
121 mounted onto slides with Canada Balsam or Permount mounting media. The slides were
122 imaged as tiled z-stacks using differential interference contrast (DIC) on an automated stage
123 at YPM-IZ (with the assistance of Daniel Drew and Eric Lazo-Wasem) and with laser point
124 confocal microscopy using a 488 nm Argon laser that excited autofluorescence in the tissues.
125 Thirty characters (defined in Appendix 2) were measured using Fiji (Collins 2007; Schindelin

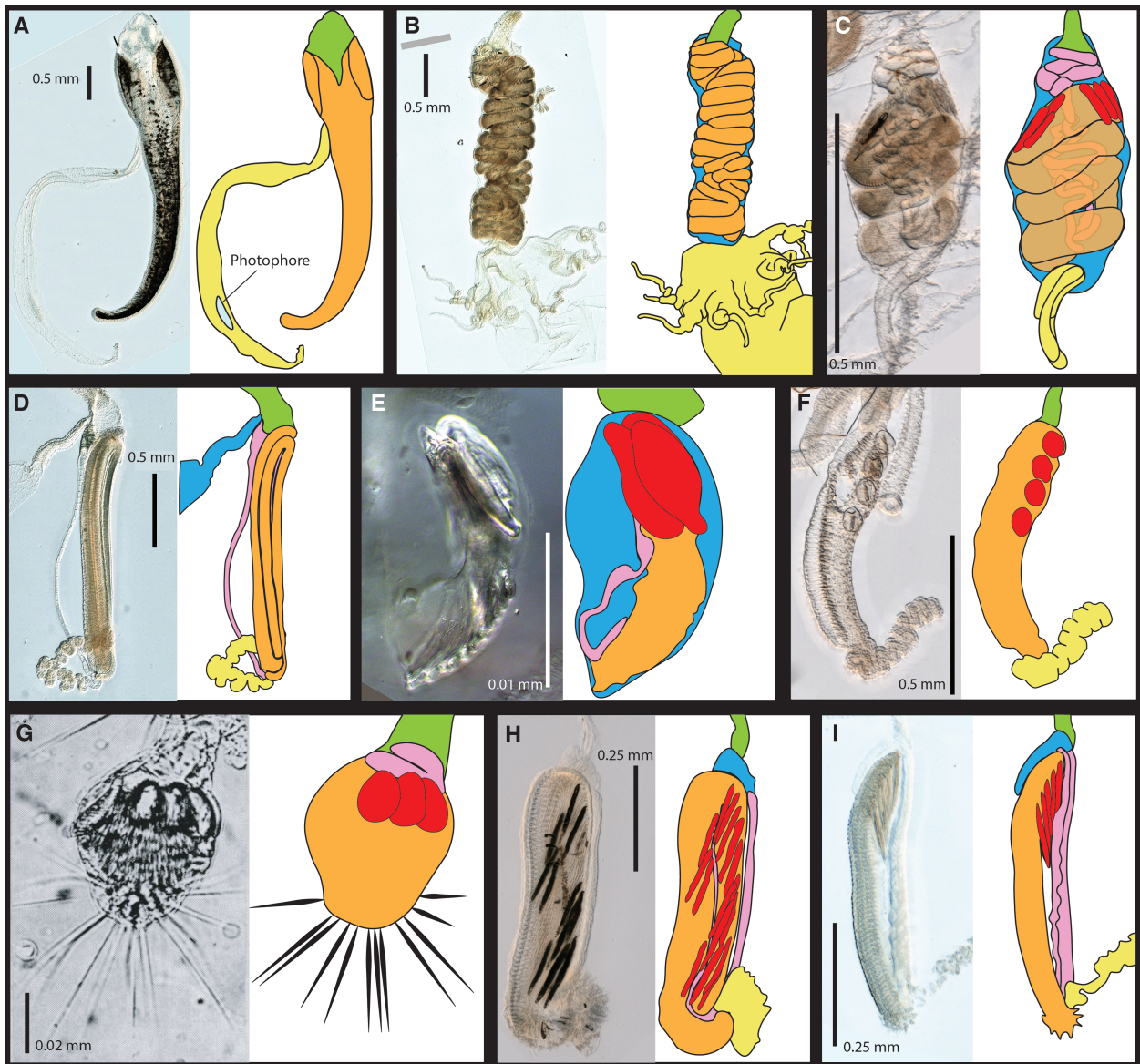


Figure 2: Tentillum diversity plate. The illustrations delineate the pedicle (green), involucrum (blue), cnidoband (orange), elastic strands (pink), terminal structures (yellow). Heteroneme nematocysts (stenoteles in C,E,F,G and mastigophores in H,I) are depicted in red for some species. A - *Erenna laciniata*, 10x. B - *Lychnagalma utricularia*, 10x. C - *Agalma elegans*, 10x. D - *Resomia ornicephala*, 10x. E - *Frillagalma vityazi*, 20x. F - *Bargmannia amoena*, 10x. G - *Cordagalma* sp., reproduced from Carré 1968. H - *Lilyopsis fluoracantha*, 20x. I - *Abylopsis tetragona*, 20x.

et al. 2012). We did not measure the lengths of contractile structures (terminal filaments, pedicles, gastrozooids, and tentacles), since they are too variable to quantify. We measured at least one specimen for 96 different species (Appendix 3, Fig. ??). Of these, we selected 38 focal species across clades based on specimen availability and phylogenetic representation. Three to five tentacle specimens from each one of these selected species were measured to capture intraspecific variation.

Siphonophore phylogeny – The phylogenetic analysis included 55 siphonophore species and 6 outgroup cnidarian species (*Clytia hemisphaerica*, *Hydra circumcincta*, *Ectopleura dumortieri*, *Porpita porpita*, *Veella veella*, *Staurocladia wellingtoni*). The gene sequences we used in this study are available online (accession numbers in Appendix 5). Some of the sequences we used were accessioned in (Dunn et al. 2005), and others we extracted from the transcriptomes in (Munro et al. 2018). Two new 16S sequences for *Frillagalma vityazi* (MK958598) and *Thermopalia* sp. (MK958599) sequenced by Lynne Christianson were included and accessioned to NCBI. We aligned these sequences using MAFFT (Katoh et al. 2002) (alignments available in Dryad). We inferred a Maximum Likelihood (ML) phylogeny (Appendix 6) from 16S and 18S ribosomal rRNA genes using IQTree (Nguyen et al. 2014) with 1000 bootstrap replicates (iqtree -s alignment.fa -nt AUTO -bb 1000). We used ModelFinder (Kalyaanamoorthy et al. 2017) implemented in IQTree v1.5.5. to assess relative model fit. ModelFinder selected GTR+R4 for having the lowest Bayesian Information Criterion score. Additionally, we inferred a Bayesian tree with each gene as an independent partition in RevBayes (Höhna et al. 2016) (Appendix 7 and 9), which was topologically congruent with the unconstrained ML tree. The *alpha* priors were selected to minimize prior load in site variation.

Given the broader sequence sampling of the transcriptome phylogeny, we ran constrained inferences (using both ML and Bayesian timetree approaches, which produced fully congruent topologies (Appendix 6 and 7)) after fixing the 5 nodes that were incongruent with the topology of the consensus tree in (Munro et al. 2018). This topology was then used to inform a Bayesian relaxed molecular clock time-tree in RevBayes, using a birth-death process (sampling probability calculated from the known number of described siphonophore species) to generate ultrametric branch lengths (Appendix 8). Scripts available in Appendix 9.

Feeding ecology – We extracted categorical diet data for different siphonophore species from published sources, including seminal papers (Biggs 1977; Purcell 1981, 1984; Andersen 1981; Mackie et al. 1987; Pugh and Youngbluth 1988; Bardi and Marques 2007), and ROV observation data (Hissmann 2005; Choy et al. 2017) with the assistance of Elizabeth Hetherington and C. Anela Choy (Appendix 10). We removed the gelatinous prey observations for *Praya dubia* eating a ctenophore and a hydromedusa, and for *Nanomia* sp. eating *Aegina*, since we believe these are rare events that have a much larger probability of being detected by ROV methods than their usual prey, and it is not clear whether the medusae were attempting to prey upon the siphonophores. Personal observations on feeding (from SHDH, CAC, and Philip Pugh) were also included for *Resomia ornicephala*, *Lychnagalma utricularia*, *Bargmannia amoena*, *Erenna richardi*, *Erenna laciniata*, *Erenna sirena*, and *Apolemia rubriversa*. In order to detect coarse-level patterns in the feeding habits, the data were merged into feeding guilds. The feeding guilds described here are: small-crustacean specialist (feeding mainly on copepods and ostracods), large crustacean specialist (feeding on large decapods, mysids, or krill), fish specialist (feeding mainly on actinopterygian larvae, juveniles, or adults), gelatinous specialist

171 (feeding mainly on other siphonophores, medusae, ctenophores, salps, and/or doliolids), and
172 generalist (feeding on a combination of the aforementioned taxa, without favoring any one
173 prey group). These were selected to minimize the number of categories while keeping the
174 most different types of prey separate. We extracted copepod prey length data from (Purcell
175 1984). To calculate specific prey selectivities, we extracted quantitative diet and zooplankton
176 composition data from (Purcell 1981), matched each diet assessment to each prey field
177 quantification by site, calculated Ivlev's electivity indices (Jacobs 1974), and averaged those
178 by species (Appendix 11).

179 *Statistical analyses* – For subsequent comparative analyses, we removed species present in
180 the tree but not represented in the morphology data, and *vice versa*. Although we measured
181 specimens labeled as *Nanomia bijuga* and *Nanomia cara*, we are not confident in some of the
182 species-level identifications, and some specimens were missing diagnostic zooids. Thus, we
183 decided to collapse these into a single taxonomic concept (*Nanomia* sp.). All *Nanomia* sp.
184 observations were matched to the phylogenetic position of *Nanomia bijuga* in the tree. We
185 carried out all phylogenetic comparative statistical analyses in the programming environment
186 R (Team 2017), using the Bayesian ultrametric species tree (Fig. 3), and incorporating
187 intraspecific variation estimated from the specimen data as standard error whenever the
188 analysis tool allowed it (Appendix 3). R scripts available in Dryad. For each character (or
189 character pair) analyzed, we removed species with missing data and reported the number of
190 taxa included. We tested each character for normality using the Shapiro-Wilk test (Shapiro
191 and Wilk 1965), and log-transformed those that were non-normal.

192 We fitted different models generating the observed data distribution given the phylogeny
193 for each continuous character using the function *fitContinuous* in the R package *geiger*
194 (Harmon et al. 2007). The models compared were the white noise (WN; non-phylogenetic
195 model that assumes all values come from a single normal distribution with no covariance
196 structure among species), the Brownian Motion (BM) model of neutral divergent evolution
197 (Martins 1996), the Early Burst (EB) model of decreasing rate of evolutionary change (Harmon
198 et al. 2010), and the Ornstein-Uhlenbeck (OU) model of stabilizing selection around a fitted
199 optimum state (Uhlenbeck and Ornstein 1930; Butler and King 2004). We then ranked the
200 models in order of increasing parametric complexity (WN,BM,EB,OU), and compared the
201 corrected Akaike Information Criterion (AICc) support scores (Sugiura 1978) to the lowest
202 (best) score, using a cutoff of 2 units to determine significantly better support. When the
203 best fitting model was not significantly better than a less complex alternative, we selected
204 the least complex model (Appendix 12). We calculated model adequacy scores using the
205 R package *arbutus* (Pennell et al. 2015) (Appendix 13). We calculated phylogenetic signal
206 in each of the measured characters using Blomberg's K (Blomberg et al. 2003) (Appendix
207 12). We reconstructed ancestral states using Maximum Likelihood (R *phytools::anc.ML*
208 (Revell 2012)), and stochastic character mapping (R *phytools::make.simmap*) for categorical
209 characters. R scripts available in Dryad.

210 In order to study the evolution of predatory specialization, we reconstructed components
211 of the diet and prey selectivity on the phylogeny using ML (R *phytools::anc.ML*). To identify
212 evolutionary associations of diet with tentillum and nematocyst characters, we compared the
213 performance of a neutral evolution model to that of a diet-driven directional selection model.
214 First, we collapsed the diet data into the five feeding guilds mentioned above (fish specialist,
215 small crustacean specialist, large crustacean specialist, gelatinous specialist, generalist), based

on which prey types they were observed consuming most frequently. Then, we reconstructed the feeding guild ancestral states using the ML function ace (package ape (Paradis et al. 2019)), removing tips with no feeding data. The ML reconstruction was congruent with the consensus stochastic character mapping (Appendix 18). Then, using the package *OUwie* (Beaulieu and O'Meara 2012), we fitted an OU model with multiple optima and rates of evolution matched to the reconstructed ancestral diet regimes, a single optimum OU model, and a BM null model, inspired by the analyses in (Cressler et al. 2015). Finally, we compared their AICc support values to select the best fitting model (Appendix 14).

To model the evolutionary associations between individual tentillum and nematocyst characters and the ability to capture particular prey types in the diet, we ran a series of phylogenetic generalized linear models (R `phyloglm`) (Appendix 17). In addition, we ran a series of comparative analyses to address hypotheses of diet-tentillum relationships posed in the literature. To test for correlated evolution among binary characters, we used Pagel's test (Pagel 1994). To characterize and evaluate the relationship between continuous characters, we used phylogenetic generalized least squares regressions (PGLS) (Grafen 1989). To compare the evolution of continuous characters with categorical aspects of the diet, we carried out a phylogenetic logistic regression (R `nlme::gls` using the 'corBrownian' function for the argument 'correlation').

In order to study correlations between the rates of evolution between different characters, we fitted a set of evolutionary variance covariance matrices (Revell and Collar 2009) (R `phytools::evol.vcv`). When fitting all covariance terms simultaneously (Appendix 19.1-20.3), we selected the largest set of characters that would allow the analysis to run without computational singularities. This excluded many of the morphometric characters which are linearly dependent on other characters. Since the functions do not tolerate missing data, we ran the analyses in two ways: One including all taxa but transforming absent states to zeroes, and another removing the taxa with absent states. To test whether phenotypic integration changes across selective regimes determined by the reconstructed feeding guilds, we carried out character-pairwise variance covariance analysis comparing alternative models (R `phytools::evolvcv.lite`), including those where correlations are the same across the whole tree and models where correlations differ between selective regimes. These analyses could only be carried out on the subset of taxa for which diet data is available, and only among character pairs that are not computationally singular for that taxonomic subset. Finally, we compared regime-specific variance covariance matrices to the general matrix and to their preceding regime matrix to identify the changes in character dependence unique to each regime (see Appendix 19). Gelatinous specialist correlations could only be estimated for a small subset of characters present in *Apolemia*, and should be interpreted with care.

To test how many times extreme nematocyst morphologies evolved, we reconstructed the ancestral states of $\log(\text{length}/\text{width})$ of the different cnidoband nematocyst types, and identified the branches with the greatest shifts. In addition to characterizing the shifts in the state values of haploneme and heteroneme elongation, we identified and located regime shifts for the rate of evolution using a Bayesian Analysis of Macroevolutionary Mixtures (BAMM) (Rabosky et al. 2014) (Appendix 16).

258 **Results**

259 *Phylogeny* – Only 5 nodes (blue dots in Figure 3) in the unconstrained inference were
260 incongruent with the (Munro et al. 2018) transcriptome tree, and these were constrained
261 during estimation of the 18S+16S tree. The topology of the constrained tree presented here
262 (Fig. 3) is congruent with the resolved nodes in (Dunn et al. 2005) and (Munro et al. 2018).

263 We retained the clade nomenclature defined in (Dunn et al. 2005) and (Munro et al.
264 2018), such as Codonophora to indicate the sister group to Cystonectae, Euphysonectae to
265 indicate the sister group to Calycophorae, Clade A and B to indicate the two main lineages
266 within Euphysonectae. In addition, we define two new clades within Codonophora (Fig. 3):
267 Eucladophora as the clade containing *Agalma elegans* and all taxa that are more closely related
268 to it than to *Apolemia lanosa*, and Tendiculophora as the clade containing *Agalma elegans* and
269 all taxa more closely related to it than to *Bargmannia elongata*. Eucladophora is characterized
270 by bearing spatially differentiated tentilla with proximal heteronemes and a narrower terminal
271 filament region. The etymology derives from the Greek *eu+kládos+phóros* for “true branch
272 bearers”. Tendiculophora are characterized by bearing rhopalonemes and desmonemes in the
273 terminal filament, having a pair of elastic strands, and developing proximally detachable
274 cnidobands. The etymology of this clade is derived from the Latin *tendicula* for “snare or
275 noose” and the Greek *phóros* for “carriers”.

276 *Evolutionary dynamics between diet and tentillum morphology* – Reconstructions of feeding
277 guilds shows that generalism is not likely to be ancestral, and it appears to have evolved at
278 least two times independently (Fig. 4). Large crustacean specialists evolve into generalists
279 twice independently, supporting hypothesis 3. Feeding guild specializations have shifted
280 from an alternative ancestral state at least five times, supporting hypothesis 2. Copepod
281 specialization and fish specialization evolved twice, and ostracod specialization evolved at
282 least once.

283 The OUwie model comparison shows that out of 30 characters, 10 show significantly
284 stronger support for the diet-driven multi-optima multi-rate OU model (Appendix 14). These
285 characters include terminal filament nematocyst size and shape, involucrum length, elastic
286 strand width, and heteroneme number. Most of these characters are found exclusively in
287 Tendiculophora, thus this may reflect processes that could be unique to this subtree. Five
288 characters including cnidoband length, cnidoband shape, and haploneme length show maximal
289 support for a diet-driven single-optimum OU model. The remaining 15 characters support
290 BM (or OU with marginal AICc difference with BM).

291 Phylogenetic logistic regressions identified evolutionary associations between individual
292 characters and the presence of particular prey types in the diet (Fig. 4, right). Shifts toward
293 ostracod presence in diet correlated with reductions in pedicle width and total haploneme
294 volume. Shifts to copepod presence in the diet were associated with reductions in haploneme
295 width, cnidoband length and width, total haploneme and heteroneme volumes, and tentacle
296 and pedicle widths. Consistently, transitions to decapod presence in the diet correlated with
297 more coiled cnidobands (Appendix 17).

298 Phylogenetic regressions of continuous characters against prey selectivity data produced
299 additional insights. Fish selectivity is associated with increased number of heteronemes
300 per tentillum, increased roundness of nematocysts (desmonemes and haplonemes), larger
301 heteronemes, reduced heteroneme/cnidoband length ratios, smaller rhopalonemes, lower

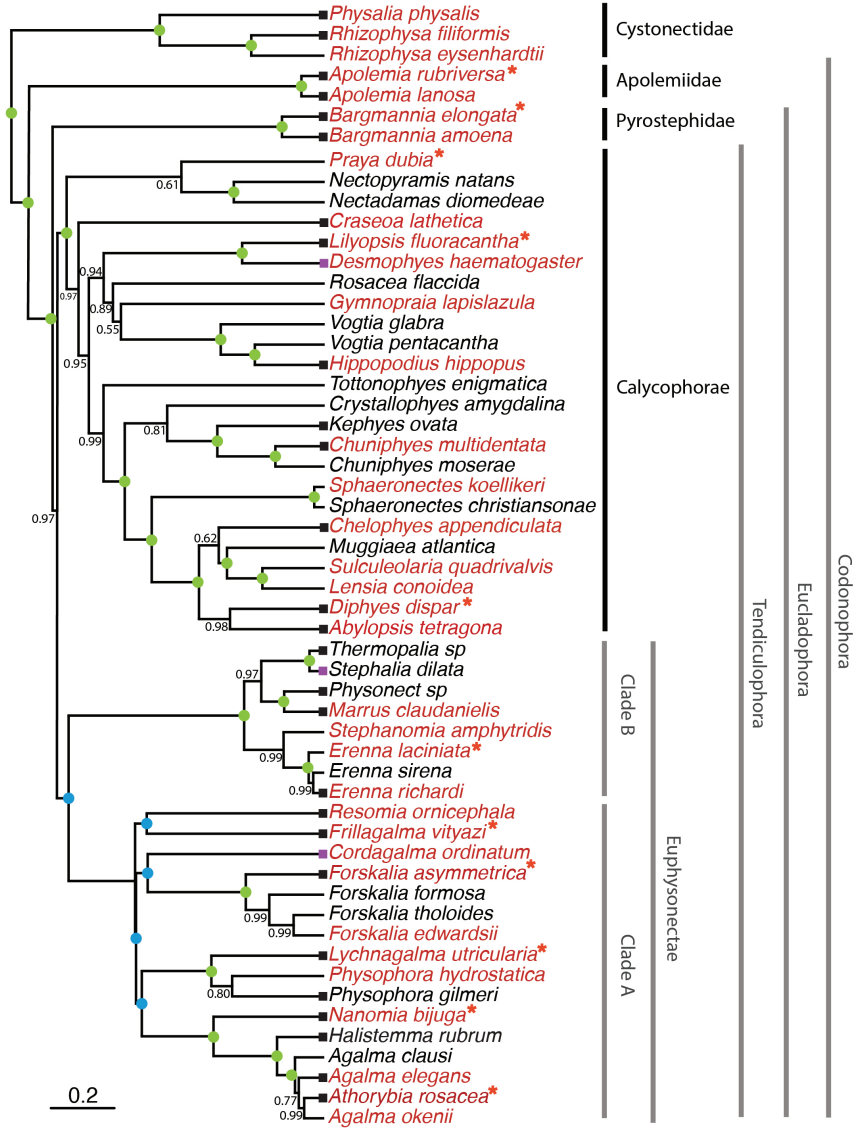


Figure 3: Bayesian time-tree built from 18S + 16S concatenated sequences. Branch lengths estimated using relaxed molecular clock. Species names in red indicate replicated representation in the morphology data. Species marked with an asterisk were recorded using high speed video. Nodes labeled with bayesian posteriors (BP). Green circles indicate BP = 1. Blue circles indicate nodes constrained to be congruent with (Munro *et al.* 2018). Tips with black squares indicate the species with transcriptomes used in (Munro *et al.* 2018). Tips with grey squares indicate genus-level correspondence to taxa included in (Munro *et al.* 2018). The main clades are labeled: in black for described taxonomic units, and in grey for operational phylogenetic designations.

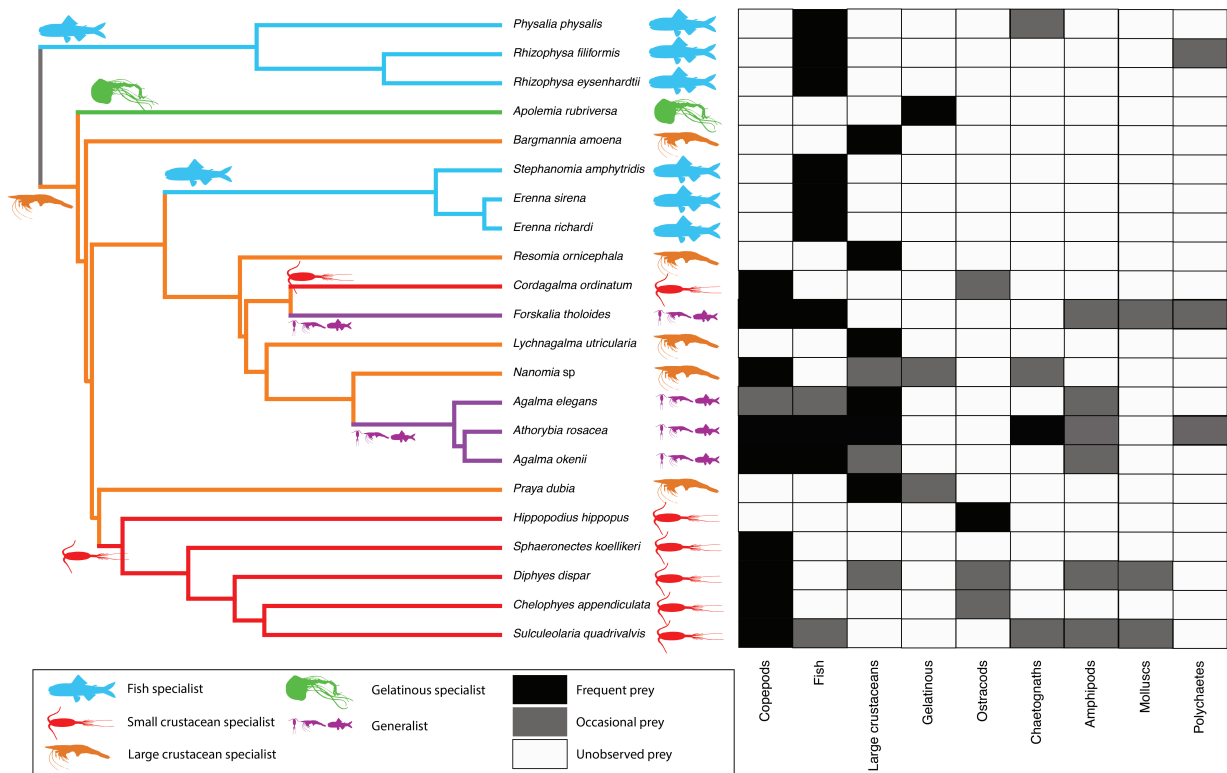


Figure 4: Left - Subset phylogeny showing the mapped feeding guild regimes that were used to inform the *OUwie* analyses. Right - Grid showing the prey items consumed from which the feeding guild categories were derived. Diet data were obtained from the literature review in Appendix 10.

haploneme SA/V ratios, and increased size of the cnidoband, elastic strand, pedicle and tentacle widths. Decapod-selective diets were associated with increasing cnidoband size and coiledness, haploneme row number, elastic strand width, and heteroneme number. Copepod-selective diets evolved in association with smaller heteroneme and total nematocyst volumes, smaller cnidobands, rounder rhopalonemes, elongated heteronemes, narrower haplonemes with higher SA/V ratios, and smaller heteronemes, tentacles, pedicles and elastic strands. Selectivity for ostracods was associated with reductions in size and number of heteroneme nematocysts, reductions in cnidoband size, number of haploneme rows, heteroneme number, and cnidoband coiledness. Heteroneme length and elongation also correlated negatively with chaetognath selectivity.

When some of the diet-morphology associations reported in the literature (Purcell 1984; Purcell and Mills 1988) were tested for correlated evolution (Table 1), we found that most were consistent with an evolutionary explanation except the relationship between terminal filament nematocysts (rhopalonemes and desmonemes) and crustaceans in the diet. The latter is likely a product of the larger species richness of crustacean-eating species with terminal filament nematocysts, rather than simultaneous evolutionary gains.

Table 1. Tests of correlated evolution between morphological characters and aspects of the diet found correlated in the literature.

Character	Aspect of diet	Test of evolutionary association	Relationship sign	P-value	Number of taxa	Association first report
Differentiated cnidobands	Hard bodied prey	Pagel's test	+	0.017	19	Purcell, 1984
Heteroneme volume	Copepod prey size	pGLS	+	0.002	8	Purcell, 1984
Terminal filament nematocysts	Crustacean diet	Pagel's test	Non-Significant	0.200	19	Purcell & Mills, 1988
Number of nematocyst types	Soft-bodied prey	Phylogenetic logistic regression	-	0.040	22	Purcell & Mills, 1988

320

321
Phenotypic integration of the tentillum – The quantitative characters we measured from tentilla and their nematocysts are highly correlated. The results indicate that the dimensionality of tentillum morphology is low, that many traits are associated with size, but that nematocyst arrangement and shape are independent of it. The variance covariance matrices (Appendix 19.1-20.2) are congruent with the abundant positive correlations observed among simple measurement characters in Fig. ??a. However, this analysis reveals more clearly the diagonal blocks that constitute the evolutionary modules, such as the heteroneme block, the terminal filament nematocyst block, and the cnidoband-pedicle-tentacle block. These results were not very sensitive to transformation of inapplicable states and taxon sampling. When we compared the rate covariance terms between characters across the different feeding guild regimes (Appendix 19.4), we found that half (48%) of the character pairs presented distinct correlation coefficients across different regimes, indicating that the mode of phenotypic integration may also shift with trophic niche. When contrasting the regime-specific rate correlation matrices to the whole-tree matrix, we were able to identify the character dependencies that are unique to each predatory niche (Appendix 19.6).

322
Under the majority of SIMMAP outcomes, large crustaceans specialists are the first regime to appear, and other regimes evolve in a shift from this ancestral specialization. Compared to the rate correlation matrix estimated over the whole tree, large crustacean specialists present strong negative correlations between haploneme elongation and heteroneme size, and between rhopaloneme elongation and tentillum size, as well as with involucrum length. With the appearance of generalists (*Forskalia* and the *Agalma-Athorybia* clade), terminal

343 filament nematocyst (desmonemes and rhopalonemes) sizes became negatively correlated with
344 the sizes of most characters, meaning that as some tentilla became larger, their individual
345 terminal nematocysts became smaller, observed to the extreme in *Agalma*. In addition,
346 heteroneme and rhopaloneme elongation became positively correlated with cnidoband size.
347 When large crustacean specialists switched to small crustacean prey in *Cordagalma* and
348 calycophorans, haploneme size became inversely correlated with heteroneme elongation,
349 which in turn developed a strong positive relationship with tentillum size. In other words, as
350 tentilla get smaller in this group, heteronemes get shorter and haplonemes get larger. The
351 extremes of this gradient can be seen in *Cordagalma* and *Hippopodius*. With the evolution
352 of fish prey specialization in cystonects and within Clade B, haploneme elongation became
353 negatively correlated with heteroneme elongation (signal driven by Clade B, since cystonects
354 lack tentacular heteronemes), and the surface area to volume ratio of haploneme nematocysts
355 switched from a strong negative relationship with cnidoband size (found in every other
356 regime) to a positively correlation. Gelatinous specialization, albeit appearing only once in
357 our tree, also carries a unique signature in character rate correlation shifts, with an increase
358 in the strength of the correlation between heteroneme shape and shaft width, consistent with
359 the appearance of birrhopaloid nematocysts with swollen shafts that are likely effective at
360 anchoring gelatinous tissue (see reference to Narcomedusae nematocysts in (Purcell and Mills
361 1988)).

362 *Evolution of nematocyst shape* – Haploneme nematocyst evolution has been mainly driven
363 by a single large shift towards elongation in Tendiculophora, which contains the majority of
364 described siphonophore species other than Cystonects, *Apolemia*, and Pyrostephidae. There
365 is one secondary return to more oval, less elongated haplonemes in *Erenna*, but it does not
366 reach the sphericity present in Cystonectae or Pyrostephidae (Fig. 5). Heteroneme evolution
367 presents a less discrete evolutionary history, where Tendiculophora evolved more elongate
368 heteronemes, but the difference between theirs and other siphonophores is much smaller than
369 the variation in shape within Tendiculophora, bearing no phylogenetic signal. In this clade,
370 evolution of heteroneme shape has diverged in both directions, and there is no correlation
371 with haploneme shape (Fig. 5), which has remained fairly constant (elongation between 1.5
372 and 2.5).

373 Haploneme and heteroneme shape share 21% of their variance across extant values,
374 and 53% of variance in their shifts along the branches of the phylogeny. However, much
375 of this correlation is due to the contrast between Pyrostephidae and their sister group
376 Tendiculophora (Fig. 3). BAMM identified a regime shift in heteroneme shape evolution on
377 the branches leading to *Agalma* and *Athorybia*. For the rates of haploneme shape evolution,
378 BAMM identified two main independent regime shifts (Fig. 5): one in the branch leading
379 to Codonophora (anisorhizas diverging from cystonects' spherical isorhizas), and one in the
380 branch leading to Clade B physonects. Clade B includes *Erenna*, *Stephanomia*, *Marrus*, and
381 rhodaliids. Most of these taxa have rod-shaped anisorhizas, but *Erenna* has oval ones). No
382 clear regime shift patterns were identified in the evolution of desmoneme and rhopaloneme
383 shape.

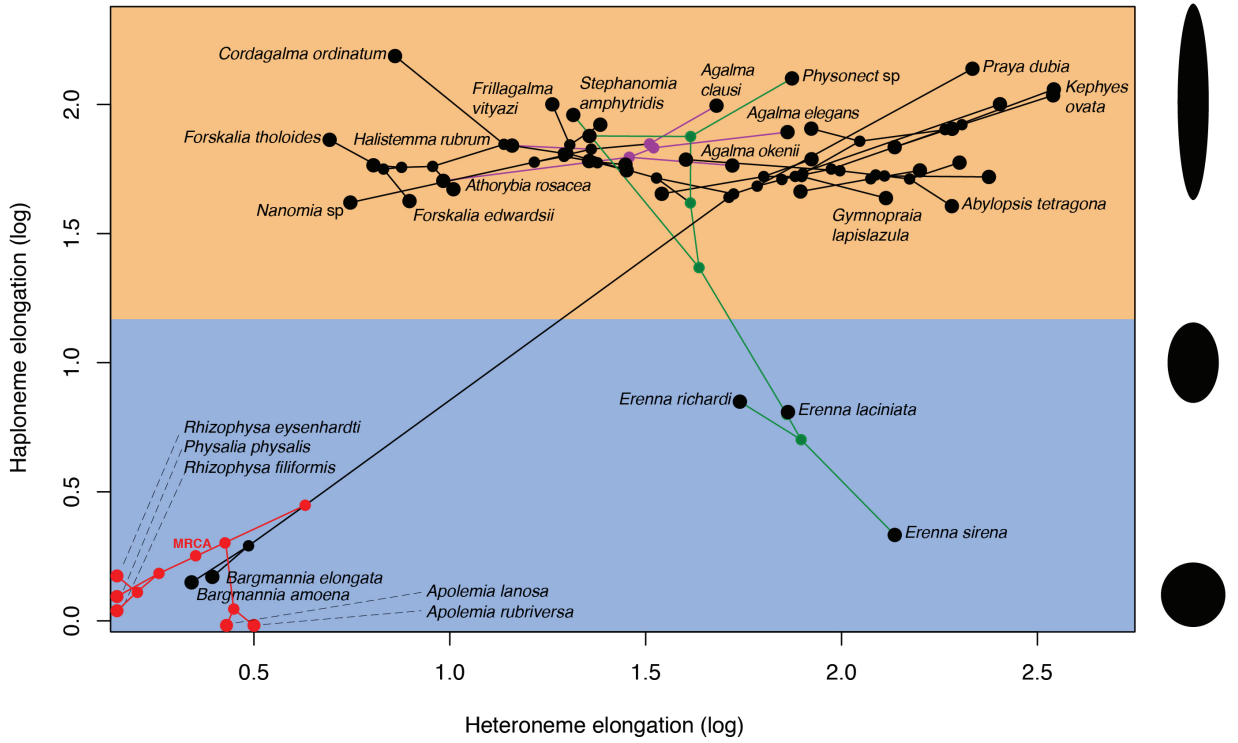


Figure 5: Phylomorphospace showing haploneme and heteroneme elongation (log scaled). Orange area delimits rod-shaped haplonemes, blue area covers oval and round shaped haplonemes. Smaller dots and lines represent phylogenetic relationships and ancestral states of internal nodes under BM. Species nodes in red were manually added to the plot. Cystonects have no tentacle heteronemes and are projected onto the haploneme axis. Apolemiids have no tentacle haplonemes and are projected onto the heteroneme axis. Colored branches and nodes correspond to BAMM regimes of accelerated haploneme shape (green) and heteroneme shape (violet) evolution.

384 **Discussion**

385 The core aims of this study are to examine the evolutionary history of siphonophore tentilla and
386 diet, characterize the evolutionary shifts in their trophic niches, and identify the morphological
387 characters that evolve with changes in prey type. We inquire whether the relationships between
388 form and function observed in extant taxa are due to correlated evolution or non-evolutionary
389 causes, whether the evolution of their trophic specializations supports or challenges traditional
390 ecological theory (such as the idea specialists evolve from generalists), and whether the diets
391 of siphonophores can be hypothesized by observing their tentacles. In addition, we produced
392 novel findings on tentillum morphology, siphonophore phylogeny, nematocyst character
393 evolution, and tentillum discharge dynamics.

394 *Evolution of tentillum morphology with diet* – Siphonophores are an abundant group of
395 zooplankton in oceanic ecosystems (Longhurst 1985; O’Brien 2007). While little is known
396 about siphonophore trophic ecology, what is known indicates that they occupy a central
397 position in midwater food webs (Choy et al. 2017), serving as trophic intermediaries between
398 smaller zooplankton and higher trophic level predators. Siphonophore species have been
399 observed to feed on a variety of prey with very different sizes, traits, and behaviors. Because
400 there is a total absence of siphonophores in the fossil record, how they became established
401 as the ubiquitous and diversified predators in today’s oceans remains an open question.
402 Predators that use morphologically similar tools for prey capture tend to capture similar prey,
403 thus their abundance and coexisting species diversity are inversely related due to competitive
404 exclusion by resource limitation (Schluter 2000). However, this is not consistent with what
405 we observe in siphonophores, which have been found to be both very abundant and locally
406 diverse (Longhurst 1985, @mapstone2014global). We hypothesize that siphonophores have
407 escaped this by specializing on different prey resources.

408 According to our reconstructions, the evolutionary history of siphonophore diets indicates
409 that being a specialist was an ancestral aspect of their trophic niche, while trophic generalism
410 is likely a derived condition. Several studies (reviewed in (Futuyma and Moreno 1988))
411 have suggested that resource specialization is an irreversible dead end due to the constraints
412 posed by phenotypic specialization. Our reconstructions show that this is not the case for
413 siphonophores, where the prey type on which they specialize has shifted at least 5 times, and
414 generalism has evolved independently at least twice. Among the evolutionary hypotheses
415 considered, we find support for both hypotheses 2 (specialist resource switching) and 3
416 (specialist to generalist), but no support for hypothesis 1 (generalist to specialist). The
417 evolutionary history of tentilla shows that siphonophores are an example of trophic niche
418 diversification via morphological innovation and evolution, which allowed transitions between
419 specialized trophic niches. This strategy is particularly important in a deep open ocean
420 ecosystem, which is a relatively homogeneous physical environment, where the primary niche
421 heterogeneity available is the potential interactions between organisms (Robison 2004).

422 One of the most common prey items found in siphonophore diets is copepods (Fig. 4).
423 Copepod-specialized diets have evolved convergently in *Cordagalma* and some calycophorans.
424 These evolutionary transitions happened together with transitions to smaller tentilla with
425 fewer cnidoband nematocysts. Tentilla are expensive single-use structures, therefore we would
426 expect that specialization in small prey would beget reductions in the size of the prey capture
427 apparatus to the minimum required for the ecological performance. *Cordagalma*’s tentilla

428 strongly resemble the larval tentilla (only found in the first-budded feeding body of the
429 colony) of their sister genus *Forskalia* spp. This indicates that the evolution of *Cordagalma*
430 tentilla could be a case of paedomorphosis associated with predatory specialization on smaller
431 prey.

432 (Purcell 1984) showed that haplonemes have a penetrating function as isorhizas in
433 cystonects and an adhesive function as anisorrhizas in Tendiculophora. The two clades that
434 have been observed primarily feeding on fish (Cystonectae and Clade B, which includes
435 *Erenna*, *Stephanomia*, *Marrus*, and rhodaliids) present an accelerated rate of haploneme
436 shape evolution towards more compact haplonemes, significantly distinct from their closest
437 relatives. Isorhizas in cystonects are known to penetrate the skin of fish during prey capture,
438 and to deliver the toxins that aid in paralysis and digestion (Hessinger 1988). *Erenna*
439 anisorrhizas are also able to penetrate human skin and deliver a painful sting (Pugh 2001)
440 (and pers. obs.), a common feature of piscivorous cnidarians like cystonects or cubozoans.

441 (Thomason 1988) hypothesized that smaller, more spherical nematocysts, with a lower
442 surface area to volume ratio, are more efficient in osmotic-driven discharge and thus have
443 more power for skin penetration. The elongated haplonemes of crustacean-eating Tendicu-
444 lophora have never been observed penetrating their crustacean prey ((Purcell 1984) and our
445 unpublished observations), and are hypothesized to entangle the prey through adhesion of
446 the abundant spines to the exoskeletal surfaces and appendages. Entangling requires less
447 acceleration and power during discharge than penetration, as it does not rely on point pressure.
448 In fish-eating cystonects and *Erenna* species, the haplonemes are much less elongated and
449 very effective at penetration, in congruence with the osmotic discharge hypothesis.

450 When we tested the diet-morphology correlation hypotheses supported in the literature
451 from a macroevolutionary perspective (Table 1), we found that most of them were consis-
452 tent with correlated evolution. The ecomorphological association between rhopalonemes,
453 desmonemes, and crustacean eaters was not congruent with a scenario of correlated evolution.
454 This is probably due to the broader set of taxa in our analyses, including multiple species
455 without desmonemes or rhopalonemes but which effectively capture crustaceans (such as
456 *Cordagalma ordinatum*, *Lychnagalma utricularia*, and *Bargmannia amoena*).

457 While our results unambiguously show that tentillum morphology evolved with diet, the
458 conclusions we can draw from these analyses are limited by the sparse dietary data available.
459 Moreover, our analyses are not sufficient to adequately test hypotheses of adaptation, since
460 that would require evidence of changes within a population exposed to different selective
461 pressures. When interpreting these results, it is important to remember that diet is a product
462 of environmental prey availability and predator selectivity. Selectivity differences across
463 siphonophore species could be driven by other phenotypes not accounted for this study. For
464 example, tentacle-deploying behavior, positioning in the water column, sensitivity thresholds
465 for nematocyst discharge, or chemical cues to ingest a captured animal. Further observations
466 on these behaviors in the field are necessary to assess their relative importance in determining
467 dietary composition. In addition to behavior, there is much biochemistry in the prey capture
468 and digestion processes that remains unexplored. Part of the success in siphonophore prey
469 capture is likely determined by the effectiveness of the toxins delivered by the nematocysts
470 on different taxa. Comparative toxin assays and venom protein evolution studies would
471 shed light on this question. Moreover, siphonophore trophic specialization may have brought
472 changes in the digestive biochemistry of gastrozooids and palpons. A comparison of the gene

473 expression levels for different enzymes in the gastrozooids of different species, together with
474 digestive enzyme sequence evolution studies, and a toxicological assay of the different venoms
475 in siphonophore nematocysts on different prey taxa, would provide a great complement to
476 our results.

477 *Generating hypotheses on siphonophore feeding ecology* – One motivation for our research
478 was to understand the links between predator capture tools and their diets so we can generate
479 hypotheses about the diets of siphonophores based on morphological characteristics. Indeed,
480 our discriminant analyses were able to distinguish between different siphonophore diets
481 based on morphological characters alone. The models produced by these analyses generated
482 testable predictions about the diets of many species for which we only have morphological
483 data of their tentacles. While the limited dataset used here is informative for generating
484 tentative hypotheses, the empirical dietary data are still scarce and insufficient to cast robust
485 predictions. This reveals the need to extensively characterize siphonophore diets and feeding
486 habits. In future work, we can test these ecological hypotheses and validate these models
487 by directly characterizing the diets of some of those siphonophore species. Predicting diet
488 using morphology is a powerful tool to reconstruct food web topologies from community
489 composition alone. In many of the ecological models found in the literature, interactions
490 among the oceanic zooplankton have been treated as a black box (Mitra 2009). The ability
491 to predict such interactions, including those of siphonophores and their prey, will enhance
492 the taxonomic resolution of nutrient-flow models constructed from plankton community
493 composition data.

494 *Phenotypic integration of siphonophore tentilla* – Many tentillum characters, such as
495 nematocysts, arose from the subfunctionalization of serial homologs (David et al. 2008). Serial
496 homologs have shared genetic elements underlying their development, and are expected to
497 have phylogenetic correlations (Wagner and Schwenk 2000). In addition, these sub-structures
498 must fit and work together in synchrony to ensnare prey successfully (functional integration).
499 Character complexes that satisfy these conditions tend to be phenotypically integrated.
500 Phenotypic integration is the set of functional and genetic correlations among the traits of an
501 organism (Pigliucci 2003). These correlations have been hypothesized to direct and constrain
502 adaptive evolution (Wagner and Schwenk 2000). The siphonophore tentillum morphospace
503 has a fairly low extant dimensionality due to an evolutionary history with many synchronous,
504 correlated changes. This is consistent with strong phenotypic integration where genetic and
505 developmental correlations are maintained by natural selection to preserve function.

506 Structural correlations within the tentillum are expected from shared regulatory networks
507 within a common developmental bud (budding tentilla in the tentacle). Similarly, correlations
508 between nematocyst subtypes are also expected given their common evolutionary and develop-
509 mental origin. None of these explanations for correlated evolution are surprising, nor require
510 natural selection. However, we also found correlations between nematocyst and tentillum
511 characters. Siphonophore tentacle nematocysts (in their cnidocytes) are not produced nor
512 matured in the developing tentillum. These cnidocytes are produced by dividing cnidoblasts
513 in the basigaster (basal swelling of the gastrozooid). Once the cnidocytes have assembled the
514 nematocyst, they migrate outward along the tentacle (Carré 1972) and position themselves
515 in the tentillum according to their type and size (Skaer 1988). Thus, the developmental pro-
516 grams that produce the observed nematocyst morphologies are spatially separated from those
517 producing the tentillum morphologies. Therefore, we hypothesize the genetic correlations and

518 phenotypic integration between tentillum and nematocyst characters are maintained through
519 natural selection on separate regulatory networks, out of the necessity to work together and
520 meet the spatial, mechanical, and functional constraints of their prey capture behavior.

521 Our evolutionary rate covariance results indicate that tentilla are not only phenotypically
522 integrated, but also show patterns of evolutionary modularity, where different sets of characters
523 appear to evolve in stronger correlations among each other than with other characters. This
524 may be indicative of the underlying genetic and developmental dependencies among closely
525 homologous nematocyst types (such as desmonemes and rhopalonemes) and structures. In
526 addition, these evolutionary modules point to hypothetical functional modules. For example,
527 the coiling degree of the cnidoband and the extent of the involucrum have correlated rates of
528 evolution, while high speed videos show that the involucrum helps direct the whiplash of the
529 uncoiling cnidoband forward (towards the prey).

530 While selection acting on character states is a widely studied phenomenon, recent studies
531 have shown that selection can also act upon the patterns of character correlations and
532 phenotypic dependencies (Young and Hallgrímsson 2005; Goswami 2006; Revell and Collar
533 2009; Monteiro and Nogueira 2010; Hallgrí'msson et al. 2012; Claverie and Patek 2013;
534 Caetano and Harmon 2018). This evolution of character relationships can allow lineages
535 to explore new regions of the morphospace and facilitate the appearance of ecological
536 novelties. Our results show that the patterns of phenotypic integration in siphonophore
537 tentilla vary among clades, and appear to display different relationships across shifting feeding
538 specializations. Similarly to what has been found in the feeding morphologies of fish (Collar
539 et al. 2005; Revell and Collar 2009), siphonophore tentilla may have accommodated new diets
540 by altering the correlations between characters. For example, changes in the size and shape
541 relationships between nematocyst types gave rise to the nematocyst complements specialized
542 in ensnaring small crustaceans or fish. Finally, the evolvability of phenotypic dependencies
543 likely had a large role in the evolution of the diverse tentilla morphologies we observe today
544 across siphonophores.

545 *Evolutionary history of tentillum morphology* – This study produced the most speciose
546 siphonophore molecular phylogeny to date, while incorporating the most recent findings
547 in siphonophore deep node relationships. This phylogeny revealed for the first time that
548 the genus *Erenna* is the sister to *Stephanomia amphytridis*. *Erenna* and *Stephanomia* bear
549 the largest tentilla among all siphonophores, thus their monophyly indicates that there was
550 a single evolutionary transition to giant tentilla. Siphonophore tentilla range in size from
551 ~30 µm in some *Cordagalma* specimens to 2-4 cm in *Erenna* species, and up to 8 cm in
552 *Stephanomia amphytridis* (Pugh and Baxter 2014). Most siphonophore tentilla measure
553 between 175 and 1007 µm (1st and 3rd quartiles), with a median of 373 µm. The extreme
554 gain of tentillum size in this newly found clade may have important implications for access
555 to large prey size classes.

556 Siphonophore tentilla are defined as lateral, monostichous evaginations of the tentacle
557 gastrovascular lumen with epidermal nematocysts (Totton and Bargmann 1965). The buttons
558 on *Physalia* tentacles were not traditionally regarded as tentilla, but (Bardi and Marques
559 2007) and our observations (Munro et al. 2018), confirm that the buttons contain evaginations
560 of the gastrovascular lumen, thus satisfying all the criteria for the definition. In this light,
561 and given that most Cystonectae bear conspicuous tentilla, we conclude (in agreement with
562 (Munro et al. 2018)) that tentilla are likely ancestral to all siphonophores, and secondarily

563 lost in *Apolemia* and *Bathyphysa conifera*.

564 The clade Tendiculophora contains far more species than its relatives Cystonectae, Apolemi-
565 idae, and Pyrostephidae. An increase in clade richness and ecological diversification can be
566 triggered by a ‘key innovation’ (Simpson 1955). The evolutionary innovation of the Tendicu-
567 lophora tentilla with shooting cnidobands and modular regions may have facilitated further
568 dietary diversification. In addition, our work identifies an interesting example of convergent
569 evolution. The region of the tentillum morphospace (Fig. ??) occupied by calycophorans was
570 independently (and more recently) occupied by the physonect *Frillagalma vityazi*. Like caly-
571 cophorans, *Frillagalma* tentilla have small C-shaped cnidobands with a few rows of anisorhizas.
572 Unlike calycophorans, they lack paired elongate microbasic mastigophores. Instead, they
573 bear three elongated stenoteles, and their cnidobands are followed by a branched vesicle,
574 unique to this genus. Their tentillum morphology is very different from that of other related
575 physonects, which tend to have long, coiled, cnidobands with many paired oval stenoteles.
576 Most studies on calycophoran diets have reported their prey to be primarily composed of
577 small crustaceans, such as copepods or ostracods (Purcell 1981, 1984). The diet of *Frillagalma*
578 *vityazi* is unknown, but this morphological convergence suggests that they evolved to capture
579 similar kinds of prey. Our DAPCs predict that *Frillagalma* has a generalist niche with both
580 soft and hard bodied prey, including copepods.

581 *Evolution of nematocyst shape* – The phylogenetic placement of siphonophores among the
582 Hydrozoa remains an unresolved question (Munro et al. 2018). The most recent work on
583 this front sets them as sister group to all other Hydroidolina (Kayal et al. 2015). Therefore,
584 there is a great uncertainty around the ancestral plesiomorphies of the common ancestor
585 of all siphonophores. This is especially true for those characters that present extreme
586 differences between Cystonectae and Codonophora (the earliest split in the siphonophore
587 phylogeny). One such character is the shape of haploneme nematocysts. A remarkable
588 feature of siphonophore haplonemes is that they are outliers to all other Medusozoa in
589 their surface area to volume relationships, deviating significantly from sphericity (Thomason
590 1988). This suggests a different mechanism for their discharge that could be more reliant on
591 capsule tension than on osmotic potentials (Carré and Carré 1980), and strong selection for
592 efficient nematocyst packing in the cnidoband (Thomason 1988; Skaer 1988). Our results
593 show that Codonophora underwent a shift towards elongation and Cystonectae towards
594 sphericity, assuming the common ancestor had an intermediate state. Since we know that
595 the haplonemes of other hydrozoan outgroups are generally spheroid, it is more parsimonious
596 to assume that cystonects retain this ancestral state. Later, we observe a return to more
597 rounded (ancestral) haplonemes in *Erenna*, concurrent with a secondary gain of a piscivorous
598 trophic niche, like that exhibited by cystonects.

599 The implications of these results to the evolution of nematocyst function are that an
600 innovation in the discharge mechanism of haplonemes may have occurred during the main shift
601 to elongation. Elongate nematocysts can be tightly packed into cnidobands. We hypothesize
602 this may be a Tendiculophora lineage-specific adaptation to packing more nematocysts into
603 a limited tentillum space, as suggested by (Skaer 1988). Tendiculophora, comprised of
604 the clades Euphysonectae and Calycophorae, includes the majority of siphonophore species.
605 Among these, are the most abundant siphonophore species, and a greater morphological and
606 ecological diversity is found. We hypothesize that this packing-efficient haploeme morphology
607 may have been a key innovation leading to the diversification of this clade. However, other

608 characters that shifted concurrently in the stem of this clade may have been responsible for
609 their extant diversity.

610 **Conclusions**

611 Siphonophores have diverse predatory niches in the open ocean, ranging from mid-trophic
612 small crustacean eaters to piscivorous super-carnivores. With the evolution of diversified
613 prey type specializations comes the evolution of morphologies adapted to the challenges
614 posed by different prey. The results presented here indicate that the associations found
615 between siphonophore tentilla and their prey are a product of correlated evolution in highly
616 integrated traits. While much of the literature focuses on how predatory generalists evolve
617 into predatory specialists, in siphonophores we find predatory specialists can evolve into
618 generalists, and that specialists on one prey type have directly evolved into specialists on
619 other prey types. Our extended morphological characterization shows that the relationships
620 between form and ecology hold across a large set of taxa and characters, and can be used to
621 generate hypotheses on the feeding habits of uncharacterized species. We conclude that the
622 siphonophores were able to become abundant oceanic predators by occupying a variety of
623 trophic niches facilitated by the evolution and diversification of extraordinary prey capture
624 tools on their tentacles.

625 **Supplementary Materials**

626 Data available from the Dryad Digital Repository: <http://dx.doi.org/10.5061/dryad.NNNN>
627 Online Appendices are available in https://github.com/dunnlab/tentilla_morph/
628 Supplementary_materials/Online_Appendices

629 **Funding**

630 This work was supported by the Society of Systematic Biologists (Graduate Student Award
631 to A.D.S.); the Yale Institute of Biospheric Studies (Doctoral Pilot Grant to A.D.S.); and
632 the National Science Foundation (Waterman Award to C.W.D., and NSF-OCE 1829835 to
633 C.W.D., S.H.D.H., and C. Anela Choy). A.D.S. was supported by a Fulbright Spain Graduate
634 Studies Scholarship.

635 **Acknowledgements**

636 We wish to thank the crew and scientists of the R/V Western Flyer, who participated in
637 the collection of many of the specimens used in this study. We also want to thank Lynne
638 Christianson and Shannon Johnson from the Monterey Bay Aquarium Research Institute
639 for their assistance in the field as well as for sequencing some of the species included in this
640 phylogeny. In addition, we wish to thank Lourdes Rojas, Daniel Drew, and Eric Lazo-Wasem
641 for their assistance in imaging the fixed specimens and managing the collections. We thank
642 Dennis Pilarczyk for organizing the prey selectivity data, Michael Landis for helping design
643 the Bayesian analyses, and Joaquin Nunez for reviewing this manuscript. Furthermore, we
644 thank Elizabeth D. Hetherington and C. Anela Choy for collating the data on siphonophore

645 feeding and for reviewing the manuscript. Finally, we thank Philip Pugh, who confirmed
646 many of our specimen identifications and taught us valuable knowledge about siphonophores.

647 References

- 648 Andersen O.G.N. 1981. Redescription of marrus orthocanna (kramp, 1942)(Cnidaria,
649 siphonophora). Zoological Museum, University of Copenhagen.
- 650 Bardi J., Marques A.C. 2007. Taxonomic redescription of the portuguese man-of-war,
651 physalia physalis (cnidaria, hydrozoa, siphonophorae, cystonectae) from brazil. Iheringia.
652 Série Zoologia. 97:425–433.
- 653 Beaulieu J., O'Meara B. 2012. OUwie: Analysis of evolutionary rates in an ou framework.
654 R package version 1.17..
- 655 Biggs D.C. 1977. Field studies of fishing, feeding, and digestion in siphonophores. Marine
656 & Freshwater Behaviour & Phy. 4:261–274.
- 657 Blomberg S.P., Garland T., Ives A.R. 2003. Testing for phylogenetic signal in comparative
658 data: Behavioral traits are more labile. Evolution. 57:717–745.
- 659 Butler M.A., King A.A. 2004. Phylogenetic comparative analysis: A modeling approach
660 for adaptive evolution. The American Naturalist. 164:683–695.
- 661 Caetano D.S., Harmon L.J. 2018. Estimating correlated rates of trait evolution with
662 uncertainty. Systematic biology. 68:412–429.
- 663 Carré D. 1972. Study on development of cnidocysts in gastrozooids of muggiaeae kochi
664 (will, 1844) (siphonophora, calycophora). Comptes Rendus Hebdomadaires des Séances de
665 l'Academie des Sciences Serie D. 275:1263.
- 666 Carré D., Carré C. 1980. On triggering and control of cnidocyst discharge. Marine &
667 Freshwater Behaviour & Phy. 7:109–117.
- 668 Choy C.A., Haddock S.H., Robison B.H. 2017. Deep pelagic food web structure as revealed
669 by in situ feeding observations. Proceedings of the Royal Society B: Biological Sciences.
670 284:20172116.
- 671 Claverie T., Patek S. 2013. Modularity and rates of evolutionary change in a power-
672 amplified prey capture system. Evolution. 67:3191–3207.
- 673 Collar D.C., Near T.J., Wainwright P.C. 2005. Comparative analysis of morphological
674 diversity: Does disparity accumulate at the same rate in two lineages of centrarchid fishes?
675 Evolution. 59:1783–1794.
- 676 Collins T.J. 2007. ImageJ for microscopy. Biotechniques. 43:S25–S30.
- 677 Costello J.H., Colin S.P., Gemmell B.J., Dabiri J.O., Sutherland K.R. 2015. Multi-jet
678 propulsion organized by clonal development in a colonial siphonophore. Nature communications.
679 6:8158.
- 680 Cressler C.E., Butler M.A., King A.A. 2015. Detecting adaptive evolution in phylogenetic
681 comparative analysis using the ornstein–uhlenbeck model. Systematic biology. 64:953–968.
- 682 David C.N., Özbek S., Adamczyk P., Meier S., Pauly B., Chapman J., Hwang J.S.,
683 Gojobori T., Holstein T.W. 2008. Evolution of complex structures: Minicollagens shape the
684 cnidarian nematocyst. Trends in genetics. 24:431–438.
- 685 Dunn C.W., Pugh P.R., Haddock S.H. 2005. Molecular phylogenetics of the siphonophora
686 (cnidaria), with implications for the evolution of functional specialization. Systematic biology.
687 54:916–935.

- 688 Futuyma D.J., Moreno G. 1988. The evolution of ecological specialization. Annual review
689 of Ecology and Systematics. 19:207–233.
- 690 Goswami A. 2006. Morphological integration in the carnivoran skull. Evolution. 60:169–
691 183.
- 692 Grafen A. 1989. The phylogenetic regression. Philosophical Transactions of the Royal
693 Society of London. B, Biological Sciences. 326:119–157.
- 694 Haddock S.H., Dunn C.W. 2015. Fluorescent proteins function as a prey attractant:
695 Experimental evidence from the hydromedusa olindias formosus and other marine organisms.
696 Biology open. 4:1094–1104.
- 697 Haddock S.H., Dunn C.W., Pugh P.R., Schnitzler C.E. 2005. Bioluminescent and red-
698 fluorescent lures in a deep-sea siphonophore. Science. 309:263–263.
- 699 Haddock S.H., Heine J.N. 2005. Scientific blue-water diving. California Sea Grant College
700 Program.
- 701 Hallgrímsisson B., Jamniczky H.A., Young N.M., Rolian C., SCHMIDT-OTT U., Marcucio
702 R.S. 2012. The generation of variation and the developmental basis for evolutionary novelty.
703 Journal of Experimental Zoology Part B: Molecular and Developmental Evolution. 318:501–
704 517.
- 705 Hardin G. 1960. The competitive exclusion principle. science. 131:1292–1297.
- 706 Harmon L.J., Losos J.B., Jonathan Davies T., Gillespie R.G., Gittleman J.L., Bryan
707 Jennings W., Kozak K.H., McPeek M.A., Moreno-Roark F., Near T.J., others. 2010. Early
708 bursts of body size and shape evolution are rare in comparative data. Evolution: International
709 Journal of Organic Evolution. 64:2385–2396.
- 710 Harmon L.J., Weir J.T., Brock C.D., Glor R.E., Challenger W. 2007. GEIGER: Investi-
711 gating evolutionary radiations. Bioinformatics. 24:129–131.
- 712 Hessinger D.A. 1988. Nematocyst venoms and toxins. The biology of nematocysts.
713 Elsevier. p. 333–368.
- 714 Hissmann K. 2005. In situ observations on benthic siphonophores (physonectae: Rhodali-
715 idae) and descriptions of three new species from indonesia and south africa. Systematics and
716 Biodiversity. 2:223–249.
- 717 Hoberg E.P., Brooks D.R. 2008. A macroevolutionary mosaic: Episodic host-switching,
718 geographical colonization and diversification in complex host–parasite systems. Journal of
719 Biogeography. 35:1533–1550.
- 720 Höhna S., Landis M.J., Heath T.A., Boussau B., Lartillot N., Moore B.R., Huelsenbeck
721 J.P., Ronquist F. 2016. RevBayes: Bayesian phylogenetic inference using graphical models
722 and an interactive model-specification language. Systematic Biology. 65:726–736.
- 723 Hutchinson G.E. 1961. The paradox of the plankton. The American Naturalist. 95:137–
724 145.
- 725 Jacobs J. 1974. Quantitative measurement of food selection. Oecologia. 14:413–417.
- 726 Johnson K.P., Malenke J.R., Clayton D.H. 2009. Competition promotes the evolution of
727 host generalists in obligate parasites. Proceedings of the Royal Society B: Biological Sciences.
728 276:3921–3926.
- 729 Kalyaanamoorthy S., Minh B.Q., Wong T.K., Haeseler A. von, Jermiin L.S. 2017. Mod-
730 elFinder: Fast model selection for accurate phylogenetic estimates. Nature methods. 14:587.
- 731 Katoh K., Misawa K., Kuma K.-i., Miyata T. 2002. MAFFT: A novel method for
732 rapid multiple sequence alignment based on fast fourier transform. Nucleic acids research.

- 733 30:3059–3066.
- 734 Kayal E., Bentlage B., Cartwright P., Yanagihara A.A., Lindsay D.J., Hopcroft R.R.,
735 Collins A.G. 2015. Phylogenetic analysis of higher-level relationships within hydroidolina
736 (cnidaria: Hydrozoa) using mitochondrial genome data and insight into their mitochondrial
737 transcription. *PeerJ*. 3:e1403.
- 738 Longhurst A.R. 1985. The structure and evolution of plankton communities. *Progress in
739 Oceanography*. 15:1–35.
- 740 Mackie G.O., Pugh P.R., Purcell J.E. 1987. Siphonophore Biology. *Advances in Marine
741 Biology*. 24:97–262.
- 742 Mapstone G.M. 2014. Global diversity and review of siphonophorae (cnidaria: Hydrozoa).
743 *PLoS One*. 9:e87737.
- 744 Martins E.P. 1996. Phylogenies, spatial autoregression, and the comparative method: A
745 computer simulation test. *Evolution*. 50:1750–1765.
- 746 Mitra A. 2009. Are closure terms appropriate or necessary descriptors of zooplankton loss
747 in nutrient–phytoplankton–zooplankton type models? *Ecological Modelling*. 220:611–620.
- 748 Monteiro L.R., Nogueira M.R. 2010. Adaptive radiations, ecological specialization, and
749 the evolutionary integration of complex morphological structures. *Evolution: International
750 Journal of Organic Evolution*. 64:724–744.
- 751 Munro C., Siebert S., Zapata F., Howison M., Serrano A.D., Church S.H., Goetz F.E.,
752 Pugh P.R., Haddock S.H., Dunn C.W. 2018. Improved phylogenetic resolution within
753 siphonophora (cnidaria) with implications for trait evolution. *Molecular Phylogenetics and
754 Evolution*.
- 755 Nguyen L.-T., Schmidt H.A., Haeseler A. von, Minh B.Q. 2014. IQ-tree: A fast and
756 effective stochastic algorithm for estimating maximum-likelihood phylogenies. *Molecular
757 biology and evolution*. 32:268–274.
- 758 O’Brien T.D. 2007. COPEPOD, a global plankton database: A review of the 2007
759 database contents and new quality control methodology..
- 760 Pagel M. 1994. Detecting correlated evolution on phylogenies: A general method for the
761 comparative analysis of discrete characters. *Proceedings of the Royal Society of London.*
762 Series B: Biological Sciences. 255:37–45.
- 763 Paradis E., Blomberg S., Bolker B., Brown J., Claude J., Cuong H.S., Desper R. 2019.
764 Package “ape”. *Analyses of phylogenetics and evolution*, version.:2–4.
- 765 Pennell M.W., FitzJohn R.G., Cornwell W.K., Harmon L.J. 2015. Model adequacy and
766 the macroevolution of angiosperm functional traits. *The American Naturalist*. 186:E33–E50.
- 767 Pigliucci M. 2003. Phenotypic integration: Studying the ecology and evolution of complex
768 phenotypes. *Ecology Letters*. 6:265–272.
- 769 Pugh P. 2001. A review of the genus erenna bedot, 1904 (siphonophora, physonectae).
770 *BULLETIN-NATURAL HISTORY MUSEUM ZOOLOGY SERIES*. 67:169–182.
- 771 Pugh P., Baxter E. 2014. A review of the physonect siphonophore genera halistemma
772 (family agalmatidae) and stephanomia (family stephanomiidae). *Zootaxa*. 3897:1–111.
- 773 Pugh P., Youngbluth M. 1988. Two new species of prayine siphonophore (calycophorae,
774 prayidae) collected by the submersibles johnson-sea-link i and ii. *Journal of Plankton Research*.
775 10:637–657.
- 776 Purcell J. 1981. Dietary composition and diel feeding patterns of epipelagic siphonophores.
777 *Marine Biology*. 65:83–90.

- 778 Purcell J.E. 1980. Influence of siphonophore behavior upon their natural diets: Evidence
779 for aggressive mimicry. *Science*. 209:1045–1047.
- 780 Purcell J.E. 1984. The functions of nematocysts in prey capture by epipelagic
781 siphonophores (coelenterata, hydrozoa). *The Biological Bulletin*. 166:310–327.
- 782 Purcell J., Mills C. 1988. The correlation of nematocyst types to diets in pelagic hydrozoa.
783 In “the biology of nematocysts”.(Eds da hessinger and hm lenhoff.) pp. 463–485..
- 784 Rabosky D.L., Grundler M., Anderson C., Title P., Shi J.J., Brown J.W., Huang H.,
785 Larson J.G. 2014. BAMM tools: An r package for the analysis of evolutionary dynamics on
786 phylogenetic trees. *Methods in Ecology and Evolution*. 5:701–707.
- 787 Revell L.J. 2012. Phytools: An r package for phylogenetic comparative biology (and other
788 things). *Methods in Ecology and Evolution*. 3:217–223.
- 789 Revell L.J., Collar D.C. 2009. Phylogenetic analysis of the evolutionary correlation using
790 likelihood. *Evolution: International Journal of Organic Evolution*. 63:1090–1100.
- 791 Robison B.H. 2004. Deep pelagic biology. *Journal of experimental marine biology and
792 ecology*. 300:253–272.
- 793 Schindelin J., Arganda-Carreras I., Frise E., Kaynig V., Longair M., Pietzsch T., Preibisch
794 S., Rueden C., Saalfeld S., Schmid B., others. 2012. Fiji: An open-source platform for
795 biological-image analysis. *Nature methods*. 9:676.
- 796 Schluter D. 2000. Ecological character displacement in adaptive radiation. *the american
797 naturalist*. 156:S4–S16.
- 798 Schmitz O. 2017. Predator and prey functional traits: Understanding the adaptive
799 machinery driving predator–prey interactions. *F1000Research*. 6.
- 800 Shapiro S.S., Wilk M.B. 1965. An analysis of variance test for normality (complete
801 samples). *Biometrika*. 52:591–611.
- 802 Simpson G.G. 1944. *Tempo and mode in evolution*. Columbia University Press.
- 803 Simpson G.G. 1955. *Major features of evolution*. Columbia University Press: New York.
- 804 Skaer R. 1988. The formation of cnidocyte patterns in siphonophores. Academic Press
805 New York.
- 806 Stireman-III J.O. 2005. The evolution of generalization? Parasitoid flies and the perils of
807 inferring host range evolution from phylogenies. *Journal of evolutionary biology*. 18:325–336.
- 808 Sugiura N. 1978. Further analysts of the data by akaike’s information criterion and the
809 finite corrections: Further analysts of the data by akaike’s. *Communications in Statistics-
810 Theory and Methods*. 7:13–26.
- 811 Team R.C. 2017. *R: A language and environment for statistical computing*. Vienna,
812 austria: R foundation for statistical computing; 2017..
- 813 Thomason J. 1988. The allometry of nematocysts. *The biology of nematocysts*. Elsevier.
814 p. 575–588.
- 815 Totton A.K., Bargmann H.E. 1965. A synopsis of the siphonophora. *British Museum
(Natural History)*.
- 816 Uhlenbeck G.E., Ornstein L.S. 1930. On the theory of the brownian motion. *Physical
review*. 36:823.
- 817 Wagner G.P., Schwenk K. 2000. Evolutionarily stable configurations: Functional in-
818 tegration and the evolution of phenotypic stability. *Evolutionary biology*. Springer. p.
819 155–217.

⁸²² Young N.M., Hallgrímsson B. 2005. Serial homology and the evolution of mammalian
⁸²³ limb covariation structure. *Evolution*. 59:2691–2704.